STATE OF OREGON
DEPARTMENT OF GEOLOGY AND MINERAL INDUSTRIES
DONALD A. HULL, STATE GEOLOGIST

GEOLOGY AND MINERAL RESOURCES MAP OF THE NAMORF QUADRANGLE, MALHEUR COUNTY, OREGON

1992

Base map by U.S. Geological Survey
Control by USGS and NOS/NOAA
Topography compiled from aerial photographs taken 1964, field checked 1987, edited 1990
Lambert Conformal Conic Projection. 1927 North American datum 10,000-foot grids based on Oregon coordinate system, south zone
1000-meter Universal Transverse Mercator grid ticks, zone 11

SCALE 1:24 000

CONTOUR INTERVAL 20 FEET
SUPPLEMENTARY CONTOUR INTERVAL 10 FEET

QUADRANGLE LOCATION

Geology by Mark L. Ferns and James P. O'Brien,
Oregon Department of Geology and Mineral Industries

Field work conducted in 1990
Reviewed by Bill Bonnichsen, Idaho Geological Survey, Moscow, Idaho, and Michael L. Cummings, Portland State University, Portland, Oregon
Cartography by Allan Cartography
Acknowledgments: The analytical discussion was prepared by Gary L. Baxter, Geochemist, Oregon Department of Geology and Mineral Industries.

TIME ROCK CHART

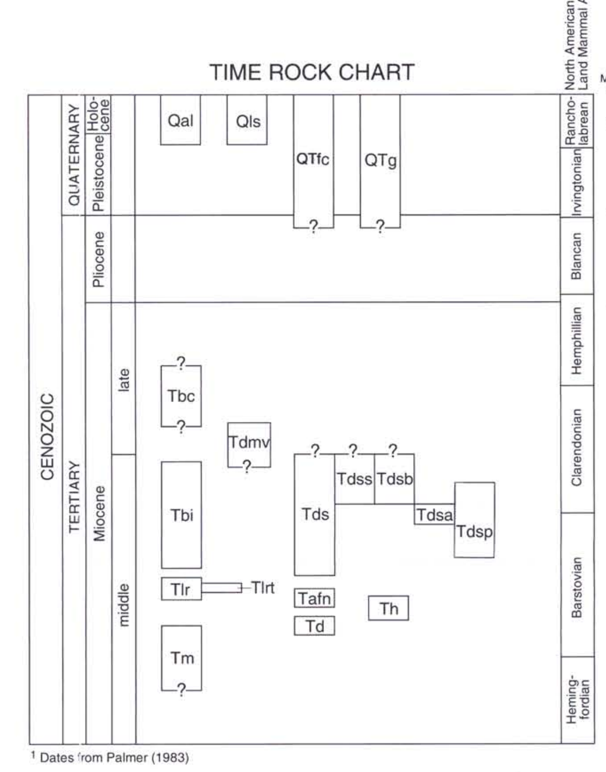

[1] Dates from Palmer (1983)

EXPLANATION

Qal — **Alluvium (Holocene and Pleistocene)** – Unconsolidated and generally poorly sorted deposits of gravel, sand, and silt accumulated along modern streams and flood plains

Qls — **Landslide deposits (Holocene and Pleistocene)** – Unconsolidated and nonstratified deposits of soil and angular blocks of rhyolite or basalt. Characterized by a hummocky topography. Slide areas along the Malheur River occur where tuffs of unit **Tafn** underlie Littlefield Rhyolite (unit **Tlr**)

QTfc — **Colluvial and alluvial fan deposits (Holocene, Pleistocene, and Pliocene?)** – Mainly alluvial fan and slope deposits consisting of unconsolidated coarse gravels and silts. Includes colluvial deposits of scree and talus along ridge slopes and accumulations of windblown silt (loess) and sand as much as 20 ft thick south of the Malheur River

QTg — **Terrace gravels (Pleistocene and Pliocene?)** – Mainly unconsolidated gravel deposits containing basalt and rhyolite clasts exposed along benches above the modern-day course of the Malheur River. Includes interbedded light-brown silts and lenticular channel gravels made up of clasts up to 2 ft in diameter from units **Tm**, **Th**, and **Tlr**

Tbc — **Bully Creek Formation (upper Miocene)** – Mainly massively bedded, pale yellowish-white and white tuffaceous siltstone with interbedded gray tuff and white diatomite. Includes light-gray, nonwelded vitric ash-flow and airfall tuff with clear glass shards and 1/2-in.-diameter white and gray inflated pumice clasts. Unit unconformably overlies an eroded surface of unit **Tds** east of Red Rock Canyon. Equivalent to the Bully Creek Formation of Kittleman and others (1965, 1967). Late Miocene age based on identification of the 9.2-Ma Devine Canyon Tuff in the Bully Creek Formation north of the map area (Walker, 1990)

Tdmv — **Mafic volcanics (middle Miocene)** – A single, dark blackish-blue aphyric basalt flow exposed in the southeast corner of the quadrangle. Laterally continuous with aphyric basalts and plagioclase-phyric basaltic andesite flows mapped by Ferns and O'Brien (unpublished map, 1989) to the south and east. Constitutes part of an areally extensive calc-alkaline volcanic field that can be traced westward from the Double Mountain quadrangle (Ramp and Ferns, 1989; Urbanczyk and Ferns, unpublished mapping, 1989). Unit unconformably overlies an eroded surface of unit **Tds** and unconformably underlies unit **Tbc**. Part of the Grassy Mountain Formation of Kittleman and others (1965, 1967)

Tbi — **Mafic intrusives (middle Miocene)** – Dark-black to grayish-black, glassy, olivine basalt dikes and sills intruded into the lower part of unit **Tds**. Typically weathers to granular slopes. Sills are characterized by upper apophyses and detached pods of glassy basalt incorporated into adjacent palagonitic country rock and were described as peperite intrusions by Weeden (1963) and Kittleman and others (1965). Coarsely crystalline interiors of the sills are coarse-grained olivine basalts (sample E, Table 1) with ophitic textures. Weeden (1963) described sills with subophitic patches of brown glass between feldspar laths. As mapped, unit includes small roof pendants of strongly silicified tuff and diatomite

Drip Springs Formation (middle Miocene) – Tuffaceous and palagonitized siltstones and sandstones, arkosic sandstones, diatomite, and basalt originally considered as being equivalent to the Deer Butte Formation (Weeden, 1961). Named by Kittleman and others (1965) for exposures at Drip Springs in the Avery Creek quadrangle to the southwest. Herein divided into four units on basis of lithologies (unit **Tds**, mainly iron-stained tuffaceous and palagonitic siltstones and sandstones that weather into angular fragments; unit **Tdss**, mainly arkose sandstones; unit **Tdsb**, basalt flows; and unit **Tdsp**, hyaloclastite deposits). Areas of alteration are designated as unit **Tdsa**

Tds — **Tuffaceous and palagonitized siltstones (middle Miocene)** – Mainly massive, silicic and tuffaceous sand- and siltstones, white to yellowish-white on fresh surfaces and weathering to orangish-yellow. Lower part of unit includes white diatomite and gray vitric tuffs with sparse feldspar crystals and silicic rock fragments. Grades upward into the characteristic yellowish-stained silicic tuffs that form erosional highs along both sides of the Malheur River. Upper part of unit **Tds** includes thin-bedded, iron-stained, white silicic tuffs that yield X-ray diffraction patterns with broadened peaks of partially disordered cristobalite, indicating conversion to a form referred to as opal-CT (Jones and Segnit, 1971). Upper part of unit to the east includes palagonitic breccias containing vesicular basalt clasts in sec. 36, T. 20 S., R. 41 E. Bedding surfaces in main area of outcrop are indistinct due to pervasive alteration. Alteration appears most intense above sills of unit **Tbi**

Tdss — **Arkosic sandstones and conglomerates (middle Miocene)** – Mainly light-brown to pale-yellow, medium- to coarse-grained, massively bedded arkosic sandstones. Interbedded with mafic flows (mapped separately as unit **Tdsb**). Petrographically, arkosic sandstones with approximately equal amounts of angular to subangular quartz and feldspar grains. Quartz grains are commonly polycrystalline and show undulose extinction. Coarse sandstones contain minor amounts of rounded and silicic volcanic, plutonic, and rare metamorphic rock fragments. Accessory minerals include biotite, muscovite, garnet, and magnetite. Exposures in the quadrangle are weakly silicified and weather to shades of yellow and reddish-orange. Unit thickens rapidly to the east, where, in the Harper quadrangle, the sandstones and interfingering basalt flows of unit **Tdsb** make up a 700-ft-thick section that unconformably overlies unit **Tdsp** (Ferns and O'Brien, 1992). The arkosic sandstones comprise the uppermost part of the Squaw Creek Formation as mapped by Weeden (1963), which was later renamed the Drip Springs Formation by Kittleman and others (1965)

Tdsb — **Basalt and basaltic andesite (middle Miocene)** – Mainly platy-jointed, vesicular, aphyric basalt flows that are locally interbedded with arkose sandstones of unit **Tdss**. Generally dark grayish-black on fresh surfaces. Basalt flow (sample F, Table 1) exposed in the NE 1/4 sec. 16, T. 21 S., R. 41 E., is approximately 40 ft thick and contains quartz xenocrysts and microphenocrysts of olivine, plagioclase, and orthopyroxene in a subophitic groundmass of clinopyroxene and glass. Exposures in the extreme southeast corner of the quadrangle can be traced to the southeast into the Keeney Ridge quadrangle, where the unit thickens and includes basaltic andesite, andesite, and tholeiitic basalt (Ferns and O'Brien, 1992). Considered by Kittleman and others (1965) to be part of the Grassy Mountain Formation

Tdsa — **Silicified siltstones and exhalative chert deposits (middle Miocene)** – Strongly silicified tuffs and thin-bedded, gray-black cherts. Includes zones of laminated exhalative chert deposits as much as 30 ft thick within thin-bedded zeolitized tuffs. Exhalative chert deposits may be due to hot-spring systems that were active after eruption of unit **Tdsp** hyaloclastite deposits. Local soft sediment folds and weakly silicified, clast-supported breccias may record penecontemporaneous downslope movement from hydrothermal vent areas

Tdsp — **Palagonitic lapilli tuffs and laharic breccias (middle Miocene)** – Reddish- and yellowish-brown palagonitic lapilli tuffs, breccias, and volcaniclastic sandstones. Mainly bedded deposits of basalt-lithic lapilli tuff with zeolitized feldspar crystals and angular to rounded clasts of basalt, silicic tuff, accretionary lapilli, and rare diatomite in a matrix of altered basaltic glass, zeolite, and calcite. Includes orangish-brown to brown, massive-matrix-supported breccias with basalt and tuff clasts and clast-supported, thin-bedded surge deposits with accretionary palagonitized lapilli. Exposures on east edge of quadrangle can be traced into the Harper quadrangle, where over 300 ft of section is exposed in a tuff cone along Cottonwood Creek (Ferns and O'Brien, 1992). Unit was probably produced by several different eruptive events

Tlr — **Rhyolite and rhyolite vitrophyre flows (middle Miocene)** – Flow sequence of at least three separate rhyolite flows. Each flow is characterized by a thick basal vitrophyre zone with horizontal flow laminations. Individual flow interiors vary from thick, columnar-jointed vitrophyre to platy-jointed lithoidal rhyolite. Distinct flow lobes with breccia carapaces are visible along the Malheur River. Margins of flow lobes and tops of individual flows are marked by vesicular vitrophyre and autoclastic breccias made up of vesicular vitrophyre blocks in an ash matrix. Irregular surface between individual flows locally filled with lenticular zones of tuffaceous siltstones and rhyolite-clast mudflow breccias. Uppermost flow surface is an east-dipping pediment with accumulations of poorly consolidated, coarse vitrophyre-clast gravels filling paleo-lows between vitrophyre outcrops. Basal flow (sample D, Table 1) on the Malheur River contains partially resorbed plagioclase, pale-green pigeonite, and opaque oxide (magnetite-ilmenite?) phenocrysts. An overlying flow north of the Malheur River (sample A, Table 1) contains plagioclase and opaque oxide phenocrysts, while the uppermost flow exposed on Squaw Creek (sample C, Table 1) contains plagioclase, augite, and opaque oxide. Also includes equant isotropic brown phenocrysts (highly altered fayalitic olivine?). Flow compositions range from metaluminous rhyodacite to rhyolite (samples A, C, and D, Table 1). The basal pigeonite-phyric flow has significantly lower abundances of zirconium and barium (sample C, Table 1) than do the stratigraphically higher rhyolites (samples A and D, Table 1). Unit has a maximum thickness of 800 ft along the Malheur River. Individual flows are as much as 300 ft thick. Equivalent to the Littlefield Rhyolite of Kittleman and others (1965) and Evans (1990a,b). Source area(s) have not yet been identified, although Evans (1990a) indicates a possible vent to the southwest. Considered to be middle Miocene in age, based on a 15.3-Ma K-Ar date on underlying unit **Td** from the Malheur River canyon to the west and a 17.5-Ma date from presumably correlative Littlefield Rhyolite flows to the southwest (Fiebelkorn and others, 1982)

Tlrt — **Tuffaceous siltstones (middle Miocene)** – Mainly yellow tuff and tuffaceous siltstones deposited on carapace tops between unit **Tlr** flows. Includes tuffaceous siltstones and coaly shales with baked plant debris at the base of the uppermost unit **Tlr** flow in the NW 1/4 sec. 5, T. 20 S., R. 41 E.

Tafn — **Ash flow tuff (middle Miocene)** – Light-gray and yellow tuff and welded tuff exposed below basal vitrophyre breccia of unit **Tlr** along the Malheur River. Ash flow is a light-yellow, partially to densely welded rhyolitic tuff with sparse potassium feldspar phenocrysts as much as 2 mm in length. Thickness of ash flow in quadrangle is about 40 ft. Unit apparently thickens to the southwest in the South Mountain quadrangle, where Evans (1990b) reports a 120-ft-thick section of tuff and welded tuff at the base of unit **Tlr**. Overlies unit **Th** and is considered by Evans (1990b) to be the base of the Littlefield Rhyolite. Petrographically distinct from the Littlefield Rhyolite flows exposed in the quadrangle and herein considered to be the distal end of a previously undescribed ash flow whose source is unknown

Th — **Icelandite flows (middle Miocene)** – Dark-bluish-gray to bluish-black, aphyric, platy-jointed icelandite (tholeiitic andesite) flows with scoria zones exposed along the Malheur River beneath unit **Tlr**. Aphyric, with a microcrystalline texture consisting of feldspar laths and intergranular clinopyroxene and opaque minerals. Chemically, a tholeiitic andesite (icelandite) characterized by low alumina and high iron (sample B, Table 1). Equivalent to Hunter Creek Basalt of Kittleman and others (1965)

Td — **Dinner Creek Tuff (middle Miocene)** – Brown to grayish-brown and yellow, welded rhyolitic ash-flow tuff that is not exposed in the quadrangle but is believed to immediately underlie unit **Th** in the northern part of the quadrangle as shown in cross-section A-A'. The ash flow immediately underlies unit **Th** half a mile west of Hog Creek Ridge near the northwest corner of sec. 19, T. 20 S., R. 41 E., in the South Mountain quadrangle (Evans, 1990b). Includes airfall and partly to densely welded lithic ash-flow tuff with at least two cooling units (Evans, 1990a,b). Chemically, unit **Td** is a high-silica peralkaline rhyolite described by Evans (1990a,b) as containing sparse plagioclase, quartz, and olivine phenocrysts. According to Haddock (1967), the ash flow thickens to the west and contains sparse anorthoclase phenocrysts

Tm — **Basalt of Malheur Gorge (middle Miocene?)** – Mostly dark-gray tholeiitic basalt flows and breccias. Includes platy-jointed and massive aphyric and plagioclase-phyric basalt and olivine basalt flows. In the quadrangle, unit **Tm** consists mainly of flow-on-flow sequence of vesicular aphyric basalt flows. Includes thin, interbedded sedimentary, hyaloclastic, and pyroclastic deposits (J. G. Evans, written communication, 1990). Includes generally holocrystalline flows with plagioclase and small olivine phenocrysts with intersertal or ophitic clinopyroxene. Equivalent to the unnamed igneous complex of Kittleman and others (1965) and named by Evans (1990a) for exposures along the Malheur River. Estimated to be over 2,000 ft thick in the Jonesboro quadrangle (Evans, 1990a)

MAP SYMBOLS

Contact – Approximately located.

Fault – Dashed where approximately located, dotted where concealed; ball and bar on downthrown side

Strike and dip of fault plane

Strike and dip of beds

Location of sample analyzed in Table 1

Location of sample analyzed in Table 2.

ISSN 0270-952X

GMS-74

Geology and Mineral Resources Map of the Namorf Quadrangle, Malheur County, Oregon

By Mark L. Ferns and James P. O'Brien

Funded jointly by the Oregon Department of Geology and Mineral Industries, the Oregon State Lottery, and the U.S. Geological Survey COGEOMAP Program as part of a cooperative effort to map the west half of the 1° by 2° Boise sheet, eastern Oregon.

MINERAL RESOURCES

Overall mineral-resource potential for the quadrangle appears low, although gold resources may occur. A sample from the exhalative chert deposits in the NW 1/4 sec. 6, T. 21 S., R. 42 E., contains trace amounts of gold and antimony (sample 12, Table 2). These cherts are interpreted as surface indicators of subaqueous hot springs. Several fault zones separating unit Tlr from unit Tds along the western edge of the quadrangle are filled with opaline quartz that in places has partially replaced vitrophyre in unit Tlr. Elevated concentrations of arsenic and antimony, along with trace amounts of gold, were detected from samples along some of the fault zones.

No other metallic or nonmetallic resources were recognized during mapping. Some of the partially opalized vitrophyre in sec. 8, T. 21 S., R. 41 E., may be of interest to rockhounds.

GROUND-WATER RESOURCES

Major springs in the quadrangle appear to be concentrated on fault lines along the western margin of the quadrangle. Potential aquifers appear to be limited to the modern alluvial deposits (unit Qal) and possibly the terrace gravels (unit QTg) along the Malheur River.

GEOCHEMISTRY

Sample Preparation

Samples for whole-rock analysis (Table 1) were crushed to minus 1/4-in. in a steel-jawed Braun chipmunk crusher and split in a Jones-type splitter in the Oregon Department of Geology and Mineral Industries (DOGAMI) laboratory. A split of about 60 g was ground to minus 200 mesh in agate media by X-ray Assay Laboratories (XRAL) of Don Mills, Ontario.

Samples for trace-element analysis of altered rocks (Table 2) were crushed to minus 1/4-in. and split as indicated above to obtain a nominal 250-g subsample. Each subsample was milled to about minus 200 mesh in chrome-steel media in an Angstrom disc mill in the DOGAMI laboratory. Each milled subsample was split again to produce two analytical samples: one to determine gold and one to determine the other trace elements.

Chemical Analysis

Whole-rock analysis: X-ray fluorescence (XRF) analyses (Table 1) were performed by XRAL. XRAL used a fused button for its analyses (1.3 g of sample roasted at 950 °C for one hour, fused with 5 g of lithium tetraborate, and the melt cast into a button). Loss on ignition (LOI) was determined from weight loss during roasting.

Trace-Element Analysis:

1. Gold – Bondar-Clegg, Ltd., of North Vancouver, British Columbia, performed the analyses for gold. The method employed was fire-assay preconcentration of the gold in a 20-g sample (gold was collected in added silver), acid dissolution of the resulting bead, and a direct current plasma (DCP) emission spectrometer finish. The detection limit was 1 part per billion (ppb).

2. Fourteen trace elements – Geochemical Services, Inc., (GSI) of Sparks, Nevada, performed the analyses for 14 trace elements. The method employed a proprietary acid dissolution/organic extraction of a 5-g sample. The finish was by induction coupled plasma (ICP) emission spectrometry. GSI considers the digestion to provide total metal contents except for gallium and thallium.

3. Eight trace elements – The DOGAMI laboratory performed the analyses for eight elements: barium, cobalt, chromium, iron, lithium, manganese, nickel, and tungsten. For the first seven elements, a 1-g sample was digested with nitric and hydrofluoric acids, the solution taken to near-dryness with perchloric acid, and the residue redissolved and taken to 100-ml volume with 10-percent nitric acid. The finish was by flame atomic absorption and (for lithium) flame emission spectrometry. The digestion provides total metal content except for barium and possibly chromium. Tungsten was determined by a method that gives semi-quantitative results: 1/4 g of sample fused with potassium pyrosulfate and dissolved with hydrochloric acid, an aliquot treated with stannous chloride and zinc dithiol, the tungsten extracted into 0.5 ml amyl acetate, and the colored complex visually compared with standards. The detection limit for tungsten was 5 ppm.

REFERENCES

Evans, J.G., 1990a, Geology and mineral resources map of the Jonesboro quadrangle, Malheur County, Oregon: Oregon Department of Geology and Mineral Industries Geological Map Series GMS-66, 1:24,000.

———1990b, Geology and mineral resources map of the South Mountain quadrangle, Malheur County, Oregon: Oregon Department of Geology and Mineral Industries Geological Map Series GMS-67, 1:24,000.

Ferns, M.L., and O'Brien, J.P., 1992, Geology and mineral resources map of the Harper quadrangle, Malheur County, Oregon: Oregon Department of Geology and Mineral Industries Geological Map Series GMS-69, scale 1:24,000.

Fiebelkorn, R.B., Walker, G.W., MacLeod, N.S., McKee, E.H., and Smith, J.G., 1982, Index to K-Ar age determinations for the state of Oregon: U.S. Geological Survey Open-File Report 82-596, 40 p.

Haddock, G.H., 1967, The Dinner Creek welded ash-flow tuff of the Malheur Gorge area, Malheur County, Oregon: Eugene, Oreg., University of Oregon doctoral dissertation, 111 p.

Jones, J.B., and Segnit, E.R., 1971, The nature of opal: I. Nomenclature and constituent phases: Journal of the Geological Society of Australia, v. 18, pt. 1, p. 57-67.

Kittleman, L.R., Green, A.R., Haddock, G.H., Hagood, A.R., Johnson, A.M., McMurray, J.M., Russell, R.G., and Weeden, D.A., 1967, Geologic map of the Owyhee region, Malheur County, Oregon: Eugene, Oreg., University of Oregon Museum of Natural History Bulletin 8, 1:125,000.

Kittleman, L.R., Green, A.R., Hagood, A.R., Johnson, A.M., McMurray, J.M., Russell, R.G., and Weeden, D.A., 1965, Cenozoic stratigraphy of the Owyhee region, southeastern Oregon: Eugene, Oreg., University of Oregon Museum of Natural History Bulletin 1, 45 p.

Palmer, A.R., 1983, The Decade of North American Geology 1983 geologic time scale: Geology, v. 11, no. 9, p. 503-504.

Ramp, L., and Ferns, M.L., 1989, Geology and mineral resources map of the Double Mountain quadrangle, Malheur County, Oregon: Oregon Department of Geology and Mineral Industries Geological Map Series GMS-58, 1:24,000.

Walker, G.W., 1990, Miocene and younger rocks of the Blue Mountains region, exclusive of the Columbia River Basalt Group and associated mafic lava flows, *in* Walker, G.W., ed., Geology of the Blue Mountains region of Oregon, Idaho, and Washington; Cenozoic geology of the Blue Mountains region: U.S. Geological Survey Professional Paper 1437, p. 101-118.

Weeden, D.A., 1961, Geology of the Harper Basin area, Oregon. Preliminary report: Unpublished report on file at Oregon Department of Geology and Mineral Industries (Malheur County), 39 p.

———1963, Geology of the Harper area, Malheur County, Oregon: Eugene, Oreg., University of Oregon master's thesis, 94 p.

Table 1. Whole-rock analyses, Namorf quadrangle, Malheur County, Oregon[1]

Map letter	Laboratory no.	1/4	1/4	Sec.	T. (S.)	R. (E.)	UTM coordinates	Elev. (ft)	Lithology	Map unit	SiO_2	Al_2O_3	TiO_2	Fe_2O_3	MnO	CaO	MgO	K_2O	Na_2O	P_2O_5	LOI	Total	Cr	Rb	Sr	Y	Zr	Nb	Ba
											Oxides (wt. percent)												Trace elements (ppm)						
A	AYB-200	SE	NE	29	20	41	4849920N 442520E	3,198	Rhyolite	Tlr	72.2	12.8	0.42	2.72	0.03	0.62	0.21	4.22	4.82	0.09	1.54	100.0	15	135	161	73	575	19	2,080
B	AYB-201	NW	SW	32	20	41	4847860N 441160E	2,640	Icelandite	Th	55.1	13.4	2.22	12.1	0.19	5.96	2.72	1.79	3.60	0.45	2.00	99.7	14	59	319	<10	238	<10	992
C	AYB-202	SW	SW	34	20	41	4847640N 444520E	2,640	Rhyolite	Tlr	68.1	12.0	0.42	5.54	0.15	1.57	0.39	4.00	4.38	0.08	2.62	99.7	15	156	150	94	563	44	2,420
D	AYB-203	SE	NW	6	21	41	4846960N 440240E	2,640	Rhyolite vitrophyre	Tlr	68.5	12.1	0.67	4.21	0.10	1.69	0.49	5.16	2.55	0.15	3.77	99.6	24	156	189	61	281	10	1,430
E	AYB-204	NW	NW	8	21	41	4845780N 441600E	3,240	Mafic sill	Tbi	46.5	16.3	1.03	9.97	0.17	9.35	8.83	0.61	2.25	0.26	4.08	99.5	135	53	379	<10	58	14	266
F	AYB-205	SE	SE	9	21	41	4844200N 444120E	3,040	Basalt	Tdsb	50.5	15.5	0.99	10.0	0.19	10.1	5.48	0.63	2.72	0.25	2.54	99.0	174	18	342	23	76	12	366

[1] XRF analyses by XRAL

Table 2. Trace-element analyses, altered rocks, Namorf quadrangle, Malheur County, Oregon[1]

Map no.	Laboratory no.	1/4	1/4	Sec.	T.(S.)	R.(E.)	UTM coordinates	Elev. (ft)	Lithology	Map unit	Ag (ppm)	As (ppm)	Au (ppb)	Cu (ppm)	Hg (ppm)	Mo (ppm)	Pb (ppm)	Sb (ppm)	Tl (ppm)	Zn (ppm)	Bi (ppm)	Cd (ppm)	Ga (ppm)	Se (ppm)	Te (ppm)	Ba (ppm)	Co (ppm)	Cr (ppm)	Fe (wt.%)	Li (ppm)	Mn (ppm)	Ni (ppm)	W (ppm)
1	AYB-100	SW	NW	33	19	41	4854560N 443520E	3,120	Opalite	Tds	<0.015	9.98	2	5.75	<0.10	1.08	2.82	<0.25	<0.5	30.1	<0.25	0.223	2.96	<1.0	<0.5	483	5.2	63	1.22	3.4	186	17	<5
2	AYB-101	NE	NE	9	20	41	4855080N 443940E	3,000	Chalcedonic breccia	Tlr	0.026	19.5	2	2.79	<0.10	1.18	6.00	0.281	<0.5	64.9	<0.25	0.272	3.12	<1.0	<0.5	741	4.7	16	1.87	5.6	303	10	<5
3	AYB-102	SE	SE	16	20	41	4852380N 444040E	2,980	Opalite breccia	Tds	0.043	10.6	2	2.52	<0.10	0.293	4.29	<0.25	<0.5	33.4	<0.25	0.167	2.61	<1.0	<0.5	392	2.4	22	0.58	0.9	139	5	<5
4	AYB-103	NE	SW	20	20	41	4851000N 441900E	3,740	Chalcedonic vein	Tlr	0.017	6.17	<1	8.76	<0.10	3.92	1.56	<0.25	<0.5	21.7	<0.25	0.150	0.949	<1.0	<0.5	45	0.5	275	2.31	3.5	794	5	<5
5	AYB-134	NW	NW	23	20	41	4852060N 446060E	2,660	Silicified tuff	Tds	0.05	20.1	<1	51.9	<0.10	3.00	5.75	1.32	<0.5	53.9	<0.25	0.196	2.97	<1.0	<0.5	648	12.4	52	4.34	14.8	612	22	<5
6	AYB-104	SW	NW	24	20	41	4851320N 447680E	2,700	Opalite	Tds	0.025	7.78	<1	8.73	<0.10	0.549	0.945	<0.25	<0.5	8.59	<0.25	<0.10	1.13	<1.0	<0.5	28	2.4	34	0.56	4.8	516	10	<5
7	AYB-105	SW	NW	27	20	41	4849460N 445260E	2,600	Silicified rhyolite breccia	Tlr	0.018	9.57	<1	3.33	<0.10	0.924	4.58	<0.25	<0.5	47.1	<0.25	<0.10	2.83	<1.0	<0.5	290	3.6	20	2.95	5.1	294	6	<5
8	AYB-106	SW	SW	34	20	41	4847600N 444500E	2,540	Silicified pyritic rhyolite breccia	Tlr	0.032	334	<1	4.08	<0.10	3.22	5.47	3.06	<0.5	114	<0.25	0.207	4.65	<1.0	<0.5	815	6.6	35	7.88	9.1	226	11	<5
9	AYB-107	SW	NW	36	20	41	4848400N 447840E	3,220	Fe-stained tuff	Tds	0.057	39.9	3	3.23	<0.10	1.17	5.05	0.591	<0.5	12.2	<0.25	0.219	2.35	<1.0	<0.5	284	3.9	12	0.47	1.6	40	4	<5
10	AYB-108	SW	SE	5	21	41	4845980N 442040E	3,320	Opalite breccia	Tds	0.036	6.36	3	4.79	<0.10	0.565	4.87	<0.25	<0.5	59.0	<0.25	0.190	3.09	<1.0	<0.5	471	4.0	42	1.35	1.9	149	5	<5
11	AYB-109	NW	SE	4	21	41	4846280N 443860E	2,840	Opalite	Tds	0.026	4.41	1	5.93	<0.10	0.751	2.13	<0.25	<0.5	42.7	<0.25	0.127	3.10	<1.0	<0.5	204	3.2	54	1.17	6.2	183	7	<5
12	AYB-110	NW	SW	3	21	41	4846360N 444620E	2,900	Opalite	Tds	0.032	3.36	<1	24.1	<0.10	3.40	0.597	<0.25	<0.5	4.39	<0.25	<0.10	<0.50	<1.0	<0.5	5	0.7	207	0.44	4.5	31	<4	<5
13	AYB-111	NE	NW	3	21	41	4847200N 445060E	2,840	Opalite	Tds	0.026	5.49	<1	3.22	<0.10	2.37	1.61	<0.25	<0.5	72.2	<0.25	<0.10	4.91	<1.0	<0.5	636	6.9	94	1.82	21.1	236	11	<5
14	AYB-116	NW	NW	31	21	42	4847200N 449540E	3,000	Ferruginous chalcedonic cherts	Tdsa	0.043	10.5	2	9.73	<0.10	3.13	4.32	0.429	<0.5	25.7	<0.25	0.102	3.99	<1.0	<0.5	308	3.5	293	1.15	109	270	10	<5
15	AYB-112	SE	NW	8	21	41	4845500N 441940E	3,400	Opalite breccia	Tds	0.024	3.18	2	4.68	<0.10	0.410	3.84	<0.25	<0.5	26.0	<0.25	0.218	1.88	<1.0	<0.5	315	2.5	34	0.87	9.0	148	6	<5
16	AYB-113	SW	NE	8	21	41	4845320N 442420E	3,200	Opalite	Tds, Tlr	0.036	3.17	<1	10.3	<0.10	0.453	1.41	<0.25	<0.5	16.4	<0.25	0.112	2.60	<1.0	<0.5	24	1.0	49	0.72	1.6	117	6	<5
17	AYB-114	NE	SE	8	21	41	4845060N 442460E	3,240	Opalite	Tds, Tlr	0.027	13.2	<1	7.11	<0.10	0.812	1.84	<0.25	<0.5	15.9	<0.25	<0.10	3.27	<1.0	<0.5	27	<0.05	80	0.67	1.4	80	5	<5
18	AYB-115	NW	NW	17	21	41	4844180N 441320E	3,440	Opalite	Tds	0.037	116	<1	13.0	<0.10	1.77	2.86	2.29	<0.5	23.5	<0.25	<0.10	3.54	<1.0	<0.5	133	4.8	33	2.01	4.5	146	11	<5

[1] Gold analyses by Bondar-Clegg; 14 elements by GSI; 8 elements by DOGAMI

GEOLOGIC CROSS SECTIONS